

# CycloZ Improves Hyperglycemia and Lipid Metabolism by Modulating Lysine Acetylation in KK-Ay Mice

Jongsu Jeon<sup>1,2,\*</sup>, Dohyun Lee<sup>1,\*</sup>, Bobae Kim<sup>1</sup>, Bo-Yoon Park<sup>3</sup>, Chang Joo Oh<sup>3</sup>, Min-Ji Kim<sup>4</sup>, Jae-Han Jeon<sup>4</sup>, In-Kyu Lee<sup>3,4</sup>, Onyu Park<sup>1,5</sup>, Seoyeong Baek<sup>1,5</sup>, Chae Won Lim<sup>6</sup>, Dongryeol Ryu<sup>7,8</sup>, Sungsoon Fang<sup>9,10</sup>, Johan Auwerx<sup>11</sup>, Kyong-Tai Kim<sup>2</sup>, Hoe-Yune Jung<sup>1,12</sup>

<sup>1</sup>R&D Center, NovMetaPharma Co., Ltd., Seoul,

<sup>2</sup>Department of Life Sciences, Pohang University of Science and Technology (POSTECH), Pohang,

<sup>3</sup>Research Institute of Aging and Metabolism, Kyungpook National University, Daegu,

<sup>4</sup>Department of Internal Medicine, Kyungpook National University Hospital, School of Medicine, Kyungpook National University, Daegu,

<sup>5</sup>School of Life Science, Handong Global University, Pohang,

<sup>6</sup>Department of Medicine, Graduate School, Daegu Catholic University, Gyeongsan,

<sup>7</sup>Department of Molecular Cell Biology, Sungkyunkwan University School of Medicine, Suwon,

<sup>8</sup>Biomedical Institute for Convergence at SKKU (BICS), Sungkyunkwan University, Suwon,

<sup>9</sup>Graduate School of Medical Science, Brain Korea 21 Project, Yonsei University College of Medicine, Seoul,

<sup>10</sup>Severance Biomedical Science Institute, Gangnam Severance Hospital, Yonsei University College of Medicine, Seoul, Korea,

<sup>11</sup>Laboratory of Integrative Systems Physiology, Institute of Bioengineering, Swiss Federal Institute of Technology in Lausanne, Lausanne, Switzerland,

<sup>12</sup>School of Interdisciplinary Bioscience and Bioengineering, Pohang University of Science and Technology (POSTECH), Pohang, Korea


**Background:** CycloZ, a combination of cyclo-His-Pro and zinc, has anti-diabetic activity. However, its exact mode of action remains to be elucidated.


**Methods:** KK-Ay mice, a type 2 diabetes mellitus (T2DM) model, were administered CycloZ either as a preventive intervention, or as a therapy. Glycemic control was evaluated using the oral glucose tolerance test (OGTT), and glycosylated hemoglobin (HbA1c) levels. Liver and visceral adipose tissues (VATs) were used for histological evaluation, gene expression analysis, and protein expression analysis.


**Results:** CycloZ administration improved glycemic control in KK-Ay mice in both prophylactic and therapeutic studies. Lysine acetylation of peroxisome proliferator-activated receptor gamma coactivator 1- $\alpha$ , liver kinase B1, and nuclear factor- $\kappa$ B p65 was decreased in the liver and VATs in CycloZ-treated mice. In addition, CycloZ treatment improved mitochondrial function, lipid oxidation, and inflammation in the liver and VATs of mice. CycloZ treatment also increased the level of  $\beta$ -nicotinamide adenine dinucleotide (NAD<sup>+</sup>), which affected the activity of deacetylases, such as sirtuin 1 (Sirt1).

**Conclusion:** Our findings suggest that the beneficial effects of CycloZ on diabetes and obesity occur through increased NAD<sup>+</sup> synthesis, which modulates Sirt1 deacetylase activity in the liver and VATs. Given that the mode of action of an NAD<sup>+</sup> booster or Sirt1 deacetylase activator is different from that of traditional T2DM drugs, CycloZ would be considered a novel therapeutic option for the treatment of T2DM.

**Keywords:** Acetylation; Diabetes mellitus, type 2; NAD; Obesity

Corresponding authors: Johan Auwerx  <https://orcid.org/0000-0002-5065-5393>  
Laboratory of Integrative Systems Physiology, Institute of Bioengineering, Swiss Federal Institute of Technology in Lausanne, CH-1015 Lausanne, Switzerland  
E-mail: admin.auwerx@epfl.ch

Kyong-Tai Kim  <https://orcid.org/0000-0001-7292-2627>  
Department of Life Sciences, Pohang University of Science and Technology (POSTECH),  
77 Cheongam-ro, Nam-gu, Pohang 37673, Korea  
E-mail: ktk@postech.ac.kr

Hoe-Yune Jung  <https://orcid.org/0000-0003-1802-5428>  
School of Interdisciplinary Bioscience and Bioengineering, Pohang University of Science and Technology (POSTECH), 77 Cheongam-ro, Nam-gu, Pohang 37673, Korea  
E-mail: elijah98@postech.ac.kr

\*Jongsu Jeon and Dohyun Lee contributed equally to this study as first authors.

Received: Jul. 20, 2022; Accepted: Nov. 3, 2022

This is an Open Access article distributed under the terms of the Creative Commons Attribution Non-Commercial License (<https://creativecommons.org/licenses/by-nc/4.0/>) which permits unrestricted non-commercial use, distribution, and reproduction in any medium, provided the original work is properly cited.

## INTRODUCTION

Type 2 diabetes mellitus (T2DM) is a metabolic disorder characterized by hyperglycemia and insulin resistance in multiple organs [1]. A healthy lifestyle that includes exercise, a proper diet, and body weight control may be beneficial in managing the disease; however, as the disease progresses, treatment with oral medications or insulin therapy is often necessary [2]. Currently available oral drugs such as hypoglycemic agents or insulin sensitizers, including sulfonylureas (SU), biguanides, thiazolidinediones (TZD), dipeptidyl peptidase-4 (DPP-4) inhibitors, and sodium-glucose cotransporter 2 (SGLT2) inhibitors have been used to control blood glucose levels for a long time [3]. However, some drugs have limited efficacy and can induce various adverse effects [4,5]. For example, patients taking SU have an increased risk of weight gain and hypoglycemia, and while those taking biguanides are exposed to a potential risk of lactic acidosis. TZDs are not recommended for patients with existing edema, heart failure, and acute liver diseases. The most common adverse reactions to DPP-4 inhibitors are upper respiratory tract infections [5,6], and while SGLT2 inhibitors are associated with urinary tract and genital infections [7]. Therefore, it is necessary to develop safer and more effective drugs with different mechanisms of action.

Lysine acetylation plays an important role in maintaining energy homeostasis in various metabolic pathways [8]. In particular, several enzymes involved in glucose and lipid metabolism are regulated by the acetylation of lysine residues [9-11]. The sirtuin family of enzymes is composed of increased the level of  $\beta$ -nicotinamide adenine dinucleotide (NAD<sup>+</sup>)-dependent deacetylases that regulate the activities of many other enzymes. Peroxisome proliferator-activated receptor gamma co-activator 1- $\alpha$  (PGC-1 $\alpha$ ), a positive regulator of mitochondrial biogenesis, is regulated by sirtuin 1 (Sirt1) [12,13]. Sirt1 also modulates the acetylation of liver kinase B1 (LKB1), a major AMP-activated kinase (AMPK) kinase involved in lipid synthesis and fatty acid oxidation [13]. Sirtuin has also been considered a new target for the treatment of chronic metabolic diseases [10] and it has been reported that the enhancement of Sirt1 activity reverts the pathologic effects of T2DM [14-16].

Young KK-Ay mice have been used as a mild hyperglycemia model for prophylactic treatment of T2DM with obesity [17]. Hyperglycemia and hyperinsulinemia in KK-Ay mice worsen with age [18]; therefore, aged KK-Ay mice with advanced hyperglycemia were used in a separate study to examine the ther-

apeutic effect of CycloZ in a severe diabetes model.

CycloZ is a combination of cyclo-His-Pro (CHP) and zinc. CHP is a cyclic dipeptide found in many tissues and has been observed to have several biological functions, such as protection against oxidative stress and anti-inflammatory activity [19]. Cyclization confers higher stability and protection against peptidases and is required for its active transport in the intestine [20] and through the blood-brain barrier [21], explaining the wide distribution of CHP throughout the body [22]. CycloZ has also been reported to improve glycemic control in diabetes via an additive mechanism [23]. However, the anti-diabetic mechanism of CycloZ is still poorly understood and needs to be better defined [24,25].

## METHODS

### Animals and administration

5 weeks of age male KK-Ay mice purchased from CLEA Japan Inc. (Nishishinbashi, Japan) were housed in individual cages in air-conditioned room at temperature of 23°C  $\pm$  3°C with a 12 hours light/dark cycle, and were free to access distilled water and laboratory chow diet. All animal experiments were approved by accordance with Ethics Review Committee of the Pohang Advanced Bio Convergence Center, Republic of Korea (ABCC201712). All animals were used for experiments after 1 week of adaptation. For prophylactic study, animals were divided into two groups. Control group was administered water as a vehicle. The KK-Ay mice were orally gavaged CycloZ (Cyclo His-Pro [5 mg/kg] and zinc gluconate [70 mg/kg]) daily for 20 weeks. For therapeutic study, the animals were divided into a control group and an experimental group at 12 weeks of age. The KK-Ay mice were orally gavaged water or CycloZ daily for 8 weeks, respectively. At the end of each experiments, all mice were anesthetized with isoflurane using RC2 Rodent Circuit Controller Anesthesia System (Vetequip, Pleasanton, CA, USA). Blood was collected by cardiac puncture and plasma was separated. Isolated adipose tissues, liver and plasma were stored at -80°C until analysis.

### Oral glucose tolerance test and glycosylated hemoglobin measurement

For oral glucose tolerance test (OGTT), mice were fasted for 16 hours and orally gavaged 2 g/kg glucose. At the time of 15, 30, 60, 90, 120 minutes after glucose administration, blood was taken from tail vein. Blood glucose level was measured immediate-

ly using a blood glucose meter (AGM-4000, Allmedicus, Anyang, Korea). To measuring glycosylated hemoglobin (HbA1c), blood was taken from tail vein. HbA1c was measured using DCA vantage® analyzer (Siemens, Munich, Germany).

#### Analysis of blood biochemical parameters

Whole blood was collected by cardiac puncture and plasma was separated by centrifugation at  $2,000 \times g$  for 10 minutes. The plasma was then stored at  $-80^{\circ}\text{C}$  until analysis. Aspartate aminotransferase (AST), alanine aminotransferase, alkaline phosphatase, total cholesterol, high-density lipoprotein cholesterol (HDL-C), low-density lipoprotein cholesterol, creatinine, and blood urea nitrogen (BUN) were measured by a biochemistry analyzer (BS-390, Mindray Bio-medical Electronics Co. Ltd., Shenzhen, China). free fatty acid was quantified by Enzy-Chrom Free Fatty Acid Assay Kit (EFFA-100, BioAssay System, Hayward, CA, USA).

#### RNA extraction, cDNA synthesis, and mRNA expression analysis

Total RNA was extracted from the tissues and cells using NucleoZOL reagent (740404.200, Macherey-Nagel, Allentown, PA, USA). An 1  $\mu\text{g}$  of total RNA was used for cDNA synthesis using iScript cDNA synthesis kit (1708891, Bio-Rad, Hercules, CA, USA). Real-time quantitative polymerase chain reaction (RT-qPCR) was performed using gene specific primers (Supplementary Table 1) and IQ SYBR Green Supermix (BR1708882, Bio-Rad). Amplification of RT-qPCR was performed as we previously described [26]. with minor modification. Briefly, RT-qPCR was performed by following reaction cycle of amplification ( $95^{\circ}\text{C}$  for 10 seconds,  $60^{\circ}\text{C}$  for 10 seconds,  $72^{\circ}\text{C}$  for 30 seconds). The expression level was normalized to those of  $\beta$ -actin or glyceraldehyde-3-phosphate dehydrogenase (*GAPDH*).

#### Quantification of $\text{NAD}^+/\beta$ -nicotinamide adenine dinucleotide

$\text{NAD}^+$  and  $\beta$ -nicotinamide adenine dinucleotide (NADH) ratio were measured by  $\text{NAD}^+/\text{NADH}$  Quantification Colorimetric Kit (K-337-100, Biovision, Milpitas, CA, USA) from the tissue lysate following the manufacturer's protocol. Briefly, 10 mg of tissues were homogenized with the provided extraction buffer. The 50  $\mu\text{L}$  of extracted samples were transferred into 96-well microplate for measuring total  $\text{NAD}^+$  concentration. To decompose NAD, the rest of extracted samples were heated to  $60^{\circ}\text{C}$  for 30 minutes. Consequently, 50  $\mu\text{L}$  of decomposed

samples were transferred into 96-well microplate. After development, the plate was measured at 450 nm.

#### Western blot

For the protein experiments, tissues and cells were lysed with radioimmunoprecipitation assay (RIPA) buffer (89901, Thermo Scientific, Waltham, MA, USA) including Halt Protease and Phosphatase Inhibitor Cocktail (78440, Thermo Scientific). For the sodium dodecyl sulfate polyacrylamide gel electrophoresis (SDS-PAGE), Bolt 4% to 12% Bis-Tris Plus Gels (Thermo Scientific) were used and the transfer was performed using Trans-Blot Turbo system (Bio-Rad). The following antibodies were used to detect the target proteins, PGC-1 $\alpha$  (NBP1-04676, Novusbio, Centennial, CO, USA), Ac-Lysine (9814S, Cell Signaling Technology [CST], Danvers, MA, USA), phospho-AMPK (5831S, CST), AMPK (2535S, CST), phospho-Akt (9271S, CST), Akt (9272S, CST), LC3 I/II (4108S, CST), GAPDH (2118S, CST), adiponectin (2789S, CST), and Sirt1 (07-131, EMD Millipore, Burlington, MA, USA).

#### Histochemistry

The liver and the adipose tissues were fixed with neutral buffered 10% formalin solution (HT-501128, Sigma, St. Louis, MO, USA) and embedded in paraffin blocks. Serial (4  $\mu\text{m}$ -thick) sections were deparaffinized, dehydrated, and stained with hematoxylin and eosin (H&E). Immunohistochemical analysis was subjected using antibodies against tumor necrosis factor  $\alpha$  (TNF $\alpha$ , Abcam, Cambridge, UK; ab1793), macrophage chemoattractant protein 1 (MCP-1, Abcam, ab25124), F4/80 (Abcam, ab111101), and CD11b (Abcam, ab133357) as described previously [27]. Stained sections were confirmed by light microscopy (Olympus BX53 upright microscope, Olympus, Tokyo, Japan).

#### Enzyme-linked immunosorbent assay

To measure concentration of insulin in plasma, Mouse insulin enzyme-linked immunosorbent assay (ELISA) kit (80-INSMS-E01, ALPCO, Salem, NH, USA) was used. To measure concentration of TNF $\alpha$  and MCP-1 in tissues, Mouse TNF $\alpha$  Quantikine ELISA Kit (MTA00B, R&D Systems, Minneapolis, MN, USA) and mouse MCP-1 Quantikine ELISA Kit (MJE00B, R&D Systems) were used. The procedure was conducted according to the manufacturer's protocol.

#### Oxygen consumption rate measurement

The oxygen consumption rate (OCR) was measured using an

XF96 Extracellular Flux Analyzer (Seahorse Bioscience, Billerica, MA, USA) according to the manufacturer's protocol. Alpha mouse liver 12 (AML12) cells were seeded in XF-96 tissue culture plates at a density of  $1 \times 10^4$  cells/well. The next day, the medium was replaced with XF base medium (pH 7.4, Seahorse Biosciences, North Billerica, MA, USA) supplemented with 25 mM D-glucose (G7528, Sigma-Aldrich), 1 mM sodium pyruvate (S8636, Sigma-Aldrich), and 1 X GlutaMAX<sup>TM</sup> (35050, Gibco, Waltham, MA, USA), followed by appropriate drugs treatment. To assess OCR, the compounds and metabolites used in this study were as follow: insulin (100 nM, I5556, Sigma-Aldrich), oligomycin A (1  $\mu$ M, 75351, Sigma-Aldrich), carbonyl cyanide 4-(trifluoromethoxy) phenylhydrazone (CCCP, 2  $\mu$ M, C2920, Sigma-Aldrich), rotenone (1  $\mu$ M, R8875, Sigma-Aldrich). To normalize by cell number, 4',6-diamidino-2-phenylindole (DAPI)-stained cells were counted automatically by ImageXpress Micro Confocal Microscopy (Molecular Devices, San Jose, CA, USA).

### MitoTracker staining

The  $0.5 \times 10^5$  cells were plated on glass coverslips in 12 well plate and incubated for 24 hours: 200  $\mu$ M of palmitate was treated with or without CycloZ in serum free media for 24 hours; 500 nM of MitoTracker Deep Red FM (M22426, Invitrogen, Carlsbad, CA, USA), diluted in serum free media, was treated and incubated for 30 minutes. Cells were washed with phosphate-buffered saline and fixed in 4% paraformaldehyde at room-temperature for 40 minutes. After Hoechst staining, the coverslips were mounted on slide glass. Images (7 to 10) per group were taken using Leica confocal laser scanning microscope. Fluorescence in randomly selected five areas in each image was measured using Leica LAS AF program (Leica, Wetzlar, Germany).

### Primer information

Primer sequences used for RT-qPCR amplification were listed in Supplementary Table 1.

### Statistical analysis

Statistical analysis was performed with the Prism software (GraphPad Prism 6, GraphPad Software Inc., San Diego, CA, USA). All data expressed as mean  $\pm$  standard error of the mean. Significance of differences between two groups were analyzed by Student's *t*-test (two-tailed), multiple comparisons were determined by one-way analysis of variance (ANOVA) followed

by Tukey's *post hoc* test.  $P < 0.05$  was considered statistically significant. We applied Grubb's test for exclusion of outliers.

## RESULTS

### CycloZ administration ameliorates T2DM and obesity in KK-Ay mice

We verified the additive effects of CycloZ in counteracting diabetes and obesity in KK-Ay mice (Supplementary Fig. 1A and B). Compared with individual compound treatment, CycloZ administration is more efficacious in improving glucose tolerance, as evaluated through the results of the OGTT and HbA1c measurements.

The weight gain of mice in the CycloZ-treated group gradually decreased compared to that of the control group at the end of the experiment without a noticeable difference in food intake (Fig. 1A, Supplementary Fig. 1C). CycloZ administration significantly suppressed the increase in the masses of the liver and visceral adipose tissue (VAT), such as epididymal adipose tissue (EAT), mesenteric adipose tissue (MAT), but not subcutaneous adipose tissue (Fig. 1B). CycloZ was safe and well-tolerated, as reflected by the absence of changes in AST, BUN, and creatinine (Supplementary Table 2).

CycloZ improved glucose tolerance in KK-Ay mice, as determined by the results of the OGTT (Fig. 1C). In addition, fasting blood glucose, HbA1c levels, and plasma insulin concentrations were significantly decreased by CycloZ administration (Fig. 1D-F). These results demonstrated that CycloZ improved glucose metabolism and insulin sensitivity.

CycloZ treatment also decreased the weights of the liver and VATs in mice. The blood lipid profile of the mice was also examined using a biochemical analyzer. It was observed that, in CycloZ-treated mice, free fatty acid and triglyceride levels were decreased, HDL-C levels were increased (Fig. 1G-I), but total cholesterol levels did not change (Supplementary Fig. 1D and E). These changes in lipid levels were explained by the decrease in the mRNA expression of genes related to fatty acid and cholesterol synthesis, including sterol regulatory-element binding transcription factor 1 (*Srebf1*), fatty acid synthase (*Fasn*), *Srebf2*, and 3-hydroxy-3-methylglutaryl-CoA reductase (*Hmgcr*) (Fig. 1K). CycloZ administration also ameliorated hepatic lipid deposition, whereas the control group showed fatty liver pathology, such as steatosis (Fig. 1L). Adiponectin level were significantly increased in the blood of CycloZ-treated mice (Fig. 1J). Moreover, the area of adipocytes in the EAT was



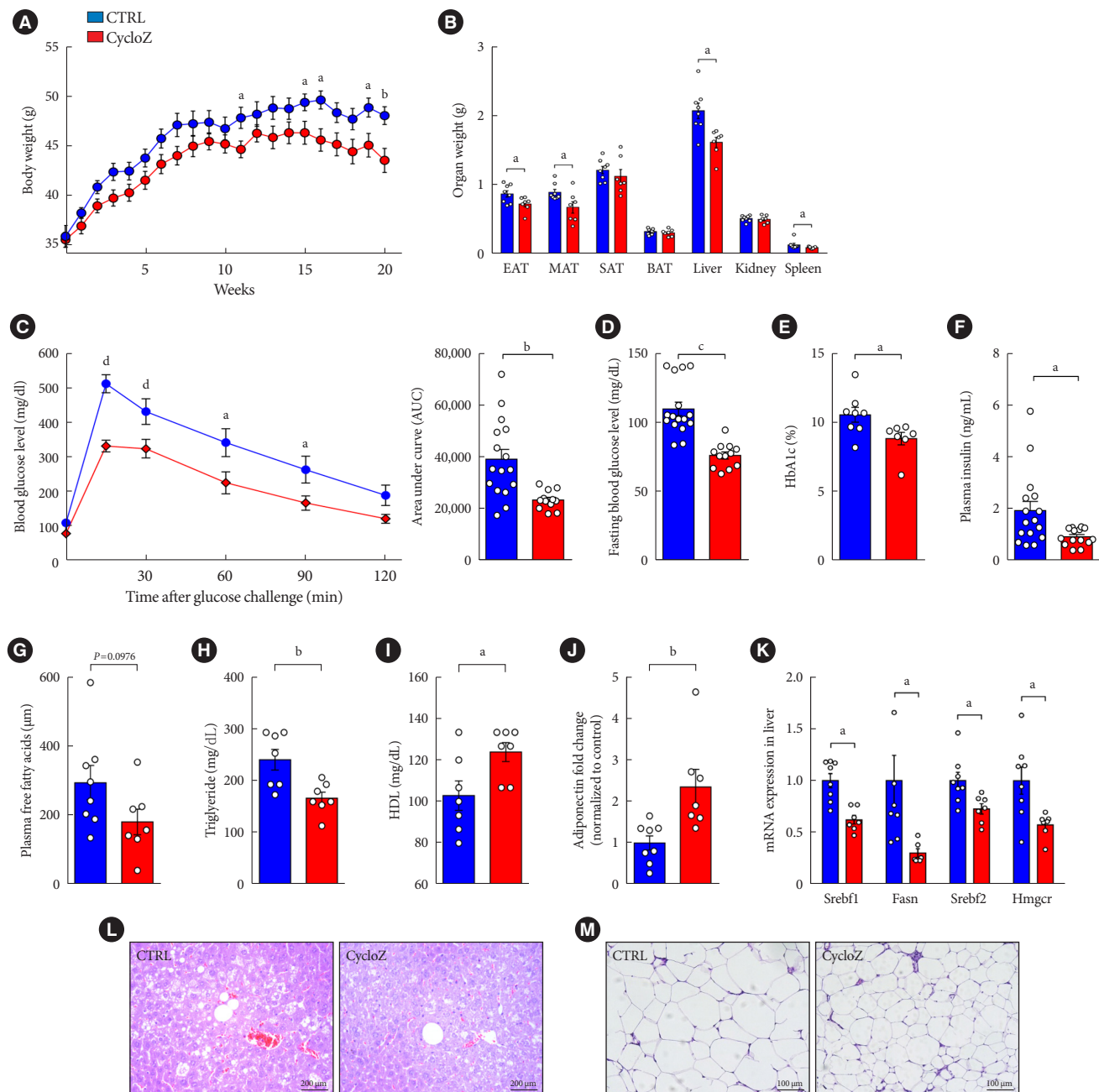


**Fig. 1.** CycloZ administration ameliorates type 2 diabetes mellitus and obese phenotypes in KK-Ay mice. (A) Body weight changes during 20 weeks of administration ( $n=7-8$ ). (B) Weight of each organ after sacrifice ( $n=7-8$ ). (C) Oral glucose tolerance test for 2 hours after 16 hours fasting and glucose administration (2 g/kg) at 10 weeks of treatment ( $n=14-16$ ). (D) Blood glucose level after 16 hours fasting at 10 weeks of treatment ( $n=14-16$ ). (E) Glycosylated hemoglobin (HbA1c) levels in KK-Ay mice at 11 weeks of treatment ( $n=7-8$ ). (F) Plasma insulin concentration ( $n=14-16$ ). (G) Plasma free fatty acid concentration ( $n=7-8$ ). (H) Plasma triglyceride concentration ( $n=7-8$ ). (I) Plasma high-density lipoprotein (HDL) concentration ( $n=7-8$ ). (J) Plasma adiponectin level was measured by Western blot ( $n=7-8$ ). (K) mRNAs expression related to fatty acid and cholesterol synthesis in liver ( $n=7-8$ ). (L, M) H&E staining of liver and epididymal adipose tissue (EAT). Data shown represent mean  $\pm$  standard error of the mean. Unpaired Student's *t*-tests. CTRL, control; MAT, mesenteric adipose tissue; SAT, subcutaneous adipose tissue; BAT, brown adipose tissue; Srebf1, sterol regulatory element-binding transcription factor; Srebf2, sterol regulatory-element binding protein; Fasn, fatty acid synthase; Hmgcr, 3-hydroxy-3-methylglutaryl-CoA reductase. <sup>a</sup> $P \leq 0.05$ , <sup>b</sup> $P \leq 0.01$ , <sup>c</sup> $P \leq 0.001$ , <sup>d</sup> $P \leq 0.0001$ .

significantly decreased in the CycloZ-treated group compared with that in the control group (Fig. 1M, Supplementary Fig. 1F). These results suggest that the weight loss induced by CycloZ administration is due to the fat reduction induced by regulating lipid and cholesterol metabolisms in the liver and VATs.

### **CycloZ improves inflammation and reduces immune cell infiltration in the liver and VATs of KK-Ay mice**

Because obesity-induced insulin resistance in the liver and VATs is closely related to chronic inflammation in many tissues, we investigated whether CycloZ reduces the production of pro-inflammatory cytokines (TNF $\alpha$  and MCP-1) and monocyte infiltration (F4/80 and CD11b). The expression of inflammatory cytokine genes in the liver and MATs, as well as the expression level of F4/80 and MCP-1, were strongly reduced by CycloZ administration (Fig. 2A). Consistently, CycloZ treatment also resulted in a significant reduction in TNF $\alpha$  and MCP-1 protein levels in the liver and EAT (Fig. 2B and C). Furthermore, expression of TNF $\alpha$ , MCP-1, F4/80, and CD11b in the liver and EAT was investigated via immunohistochemistry (Fig. 2D and E). Both inflammatory cytokine production and monocyte infiltration were abolished by CycloZ administration. Taken together, these data suggest that the improvement in tissue insulin resistance after CycloZ administration was accompanied by reduced inflammation.

### **CycloZ administration improves mitochondrial biogenesis and inflammation by modulating protein acetylation levels**

Infiltrating macrophages play an important role in developing of insulin resistance in metabolic organs. Their activity is partly regulated by the deacetylation of transcription factors, such as the p65 subunit of nuclear factor- $\kappa$ B (NF- $\kappa$ B) [28]. Our results showed that CycloZ robustly reduced the acetylation of p65 in the liver and EATs of CycloZ-treated mice (Fig. 3A).

Lysine acetylation regulates the activities of many metabolic enzymes and transcription factors. In previous studies, the global lysine acetylation profile was found to be increased in the kidneys and hearts of patients with diabetes [29,30]. In the study, we found that the global acetyl-lysine level in the liver of mice in the CycloZ-treated group was significantly reduced compare to that in the control group (Supplementary Fig. 2A). Moreover, the acetylation of PGC-1 $\alpha$  and LKB1 was significantly reduced in the liver and EATs of CycloZ-treated mice (Fig. 3B and C). In addition to its deacetylation, PGC-1 $\alpha$  requires AMPK-mediated phosphorylation for activation.

Therefore, we examined whether CycloZ affected the AMPK-PGC-1 $\alpha$  pathway. Our results showed that AMPK phosphorylation was increased in the livers and EATs of CycloZ-treated mice (Fig. 3D).

Next, we examined the expression of PGC-1 $\alpha$ -related genes. The expression of forkhead box O1 (*Foxo1*), estrogen-related receptor alpha (*Esrra*), transcription factor A, mitochondrial (*Tfam*), nuclear respiratory factor 1 (*Nrf1*), and uncoupling protein 1 (*Ucp1*), which are required for the mitochondrial biogenesis, were increased in the livers and MATs of mice in the CycloZ-treated group compared to those in the control group (Fig. 3E). Similarly, the expressions of peroxisome proliferator-activated receptor alpha (*Ppara*), carnitine palmitoyl-transferase 1A (*Cpt1a*), and PPARG coactivator 1 alpha (*Ppargc1a*), which are related to lipid oxidation in the liver, were also increased in the CycloZ-treated group, and acyl-CoA oxidase 1 (*Acox1*), medium-chain acyl-CoA dehydrogenase (*Mcad*), *Ppara*, *Cpt1a*, and *Ppargc1a* levels were increased in the MATs of CycloZ-treated mice (Fig. 3F). Moreover, increased mitochondrial biogenesis upon CycloZ administration was demonstrated by the increased mitochondrial DNA (mtDNA) content in the livers of CycloZ-treated mice (Supplementary Fig. 2B).

This suggests that CycloZ improves mitochondrial biogenesis, which increases mitochondrial function, and the activation of lipid oxidation. Therefore, we investigated mitochondrial respiration and, OCR in AML12 mouse hepatocytes. Compared with the palmitate-treated group, the CycloZ-treated group showed significantly enhanced OCR, ATP-linked respiration, and maximal respiration capacity (Fig. 3G). MitoTracker Deep Red FM staining showed an increased mitochondrial mass in CycloZ-treated AML12 cells (Fig. 3H). These results demonstrate that CycloZ enhances mitochondrial biogenesis and function by modulating acetylation status.

### **CycloZ administration regulates the expression of genes involved in NAD<sup>+</sup> synthesis**

We observed the deacetylation of the non-histone transcription factors, PGC-1 $\alpha$ , LKB1, and p65 in the liver and VATs. The sirtuin family of deacetylases is known to regulate the acetylation of the above proteins. Sirt1 has the broadest spectrum of substrates and affects various physiological pathways, including energy metabolism [31]. Since Sirt1 uses NAD<sup>+</sup> as a co-substrate to remove acetyl groups, the cellular NAD<sup>+</sup>/NADH ratio reflects Sirt1 enzyme activity [10,32]. Therefore, we hy-

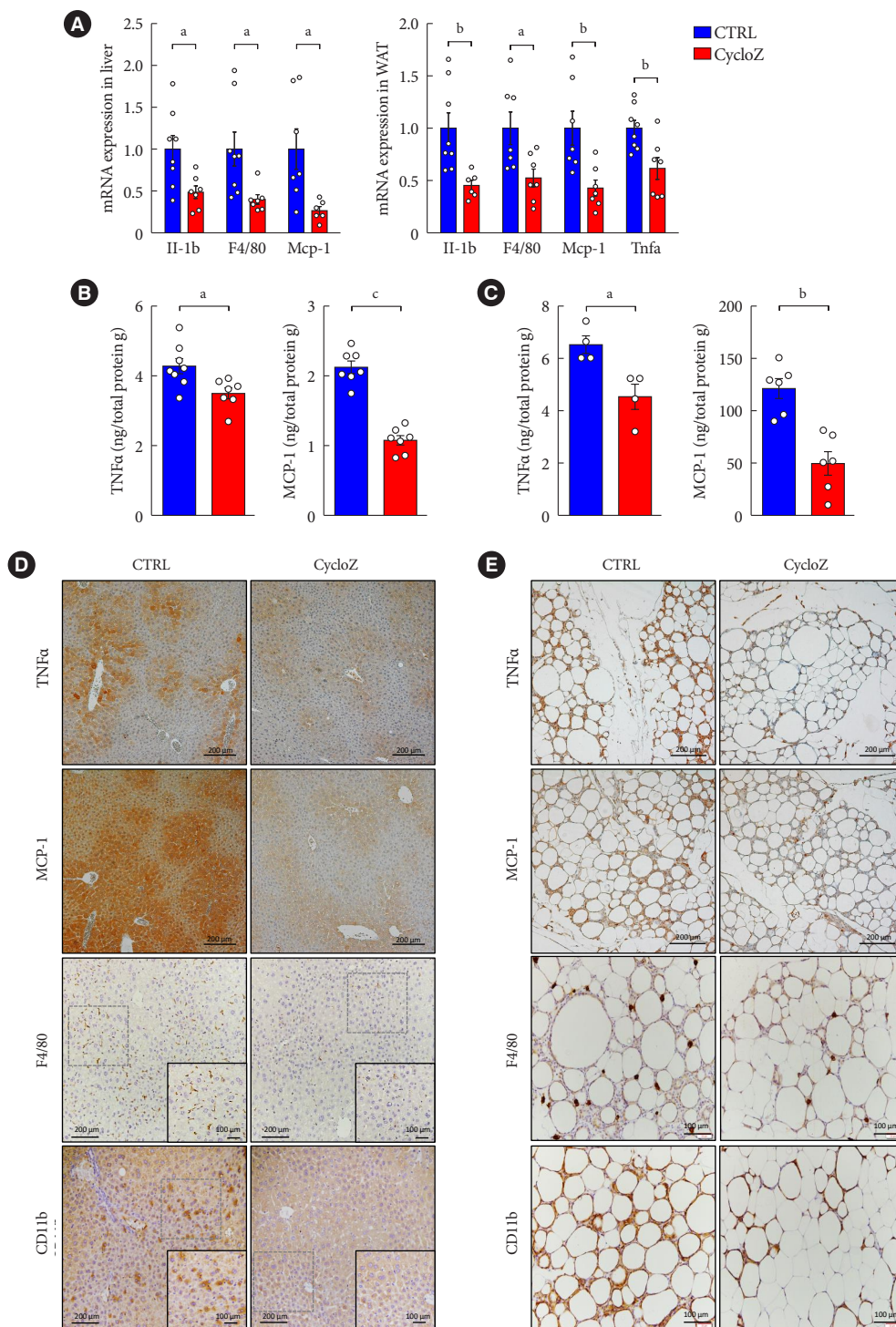


**Fig. 2.** CycloZ recovers inflammation and immune cell infiltration in liver and visceral adipose tissues of KK-Ay mice. (A) mRNAs expression level related inflammatory cytokines and infiltrated monocyte in liver and mesenteric adipose tissue ( $n=7-8$ ). (B, C) Tumor necrosis factor  $\alpha$  (TNF $\alpha$ ) and macrophage chemoattractant protein 1 (MCP-1) protein levels in liver (B) and epididymal adipose tissue (EAT) (C) ( $n=7-8$ ). (D, E) Expression of TNF $\alpha$ , MCP-1, F4/80, and CD11b in liver (D) and EAT (E) was measured by immunohistochemistry. Data shown represent mean  $\pm$  standard error of the mean. Unpaired Student's  $t$ -tests. CTRL, control; IL-1b, interleukin 1 beta; WAT, white adipose tissue. <sup>a</sup> $P \leq 0.05$ , <sup>b</sup> $P \leq 0.01$ , <sup>c</sup> $P \leq 0.0001$ .

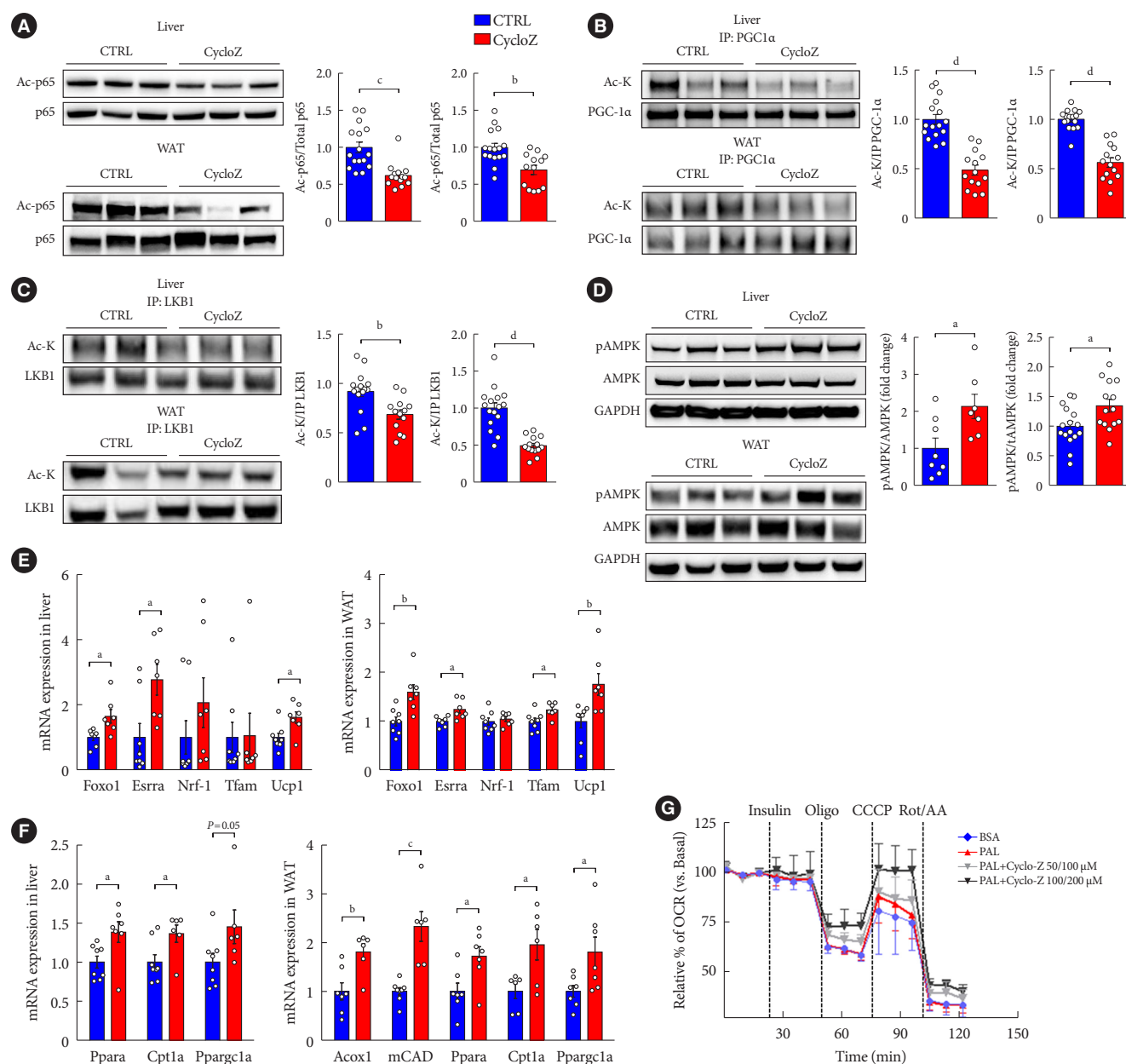


**Fig. 3.** CycloZ improves mitochondrial function via sirtuin 1 deacetylase. (A) Levels of acetylated lysine on p65 in liver and white adipose tissue (WAT) ( $n=14-16$ ). (B) Acetylated lysine levels on peroxisome proliferator-activated receptor gamma coactivator 1-alpha (PGC-1 $\alpha$ ) in liver and epididymal adipose tissue (EAT) ( $n=14-16$ ). (C) Acetylated lysine levels on liver kinase B1 (LKB1) in liver and EAT ( $n=14-16$ ). (D) Phosphorylated AMP-activated kinase (AMPK) (T172) in liver and EAT ( $n=7-8$ ). (E) mRNAs expression level related to mitochondrial biogenesis in liver and mesenteric adipose tissue (MAT) ( $n=7-8$ ). (F) mRNAs expression level related to lipid oxidation in liver and MAT ( $n=7-8$ ). (G) Oxygen consumption rate (OCR) was measured in alpha mouse liver 12 (AML12) after 16-hour treatment of CycloZ with and without palmitate. (H) MitoTracker staining for measuring mitochondrial mass. Data shown represent mean  $\pm$  standard error of the mean. Unpaired Student's  $t$ -tests. CTRL, control; IP, immunoprecipitation; Ac-K, acetylated-lysine; GAPDH, glyceraldehyde-3-phosphate dehydrogenase; Foxo1, forkhead box O1; Esrra, estrogen related receptor alpha; Nrf1, nuclear respiratory factor 1; Tfam, transcription factor A, mitochondrial; Ucp1, uncoupling protein 1; Ppara, peroxisome proliferator-activated receptor alpha; Cpt1a, carnitine palmitoyltransferase 1A; Ppargc1a, PPARG coactivator 1 alpha; CCCP, carbonyl cyanide 4-(trifluoromethoxy) phenylhydrazone; Rot/AA, rotenone/antimycin A; BSA, bovine serum albumin; PAL, palmitic acid. <sup>a</sup> $P \leq 0.05$ , <sup>b</sup> $P \leq 0.01$ , <sup>c</sup> $P \leq 0.001$ , <sup>d</sup> $P \leq 0.0001$ . (Continued to the next page)



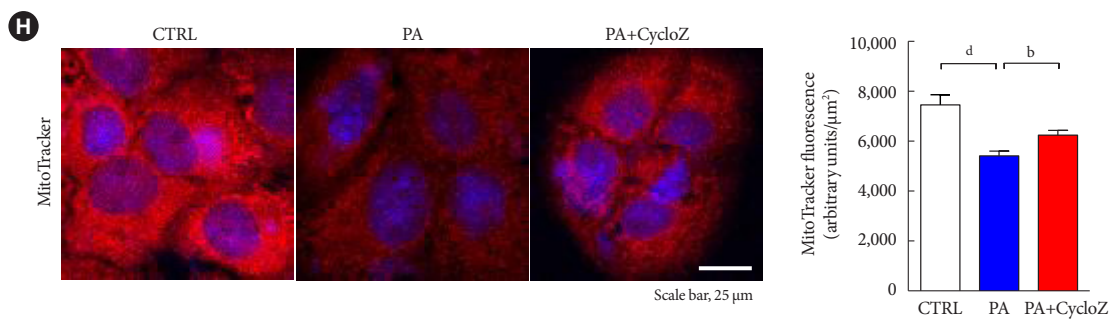


Fig. 3. Continued.

pothesized that CycloZ increases the deacetylation activity of Sirt1 by increasing  $\text{NAD}^+$  levels or the  $\text{NAD}^+/\text{NADH}$  ratio.

We found that the  $\text{NAD}^+/\text{NADH}$  ratio was elevated by CycloZ administration in the liver and EAT, but not in the muscle (Fig. 4A, Supplementary Fig. 2C). The increase in  $\text{NAD}^+/\text{NADH}$  ratio in the liver and EAT was due to an increase in the total amount of  $\text{NAD}^+$  (Fig. 4B). To investigate the reason for this increase in  $\text{NAD}^+$  level, we examined the expression of genes involved in  $\text{NAD}^+$  synthesis. The results showed that the expression of several genes involved in  $\text{NAD}$  biosynthesis was significantly upregulated upon CycloZ administration relative to the control group (Fig. 4C and D). These results suggest that CycloZ increased  $\text{NAD}^+$  levels by modulating gene expression related to  $\text{NAD}^+$  synthesis.

#### Therapeutic CycloZ administration improves glucose control in a mouse model of severe T2DM

The *in vivo* data we reported so far showed the prophylactic effects of CycloZ in KK-Ay mice that were administered the drug at early time points in their progression to hyperglycemia. In the clinical setting, patients with T2DM are only started on drugs when they are diagnosed with pre-diabetes or diabetes. Therefore, it is necessary to examine the therapeutic effect of CycloZ in the later stages of diabetes, which is typically characterized by severe hyperglycemia. According to a study by Iwatsuka et al. [18], KK-Ay mice exhibit an age-dependent increase in hyperglycemia and insulin resistance. By measuring HbA1c levels in KK-Ay mice, we found that hyperglycemia became more severe at 12 weeks of age compared to that of 8 weeks of age (Supplementary Fig. 3A). Therefore, we investigated the therapeutic effect of CycloZ by administering it for 8 weeks in mice that are 12 weeks of age. Glucose tolerance (Fig. 5A) and HbA1c levels (Fig. 5B) were significantly improved by CycloZ administration. Moreover, we also observed the re-

duced acetylation of PGC-1 $\alpha$  and LKB1 and increased AMPK phosphorylation were also evident and fully consistent with the results of the prophylactic study (Fig. 5C and D, Supplementary Fig. 3G). Likewise, the expression of mRNAs related to mitochondrial biogenesis and function were also increased in the liver after the therapeutic administration of CycloZ (Supplementary Fig. 3E and F). In addition, the amount of  $\text{NAD}^+$ ,  $\text{NAD}^+/\text{NADH}$  ratio and expression of genes involved in  $\text{NAD}^+$  synthesis were also increased upon CycloZ administration under these conditions (Fig. 5E and F). These results suggest that CycloZ administration is still effective even in a more severe diabetes model.

## DISCUSSION

The metabolism of some trace elements such as zinc, copper, chromium, and manganese, has been reported to be altered in patients with T2DM [33]. Among these elements, zinc levels are particularly reduced in the blood and various organs, including the liver, muscle, adipose tissue, and pancreas [33,34]. In animal studies, zinc deficiency exacerbates insulin resistance by modulating the activity of enzymes involved in insulin signaling, such as protein tyrosine phosphatase 1B (PTP1B), phosphatase and tensin homolog (PTEN), and tribbles homolog 3 (TRB3) [35]. Studies on the mode of action of CycloZ have mainly focused on its effect on increasing zinc levels. Indeed, CycloZ was reported to chelates zinc ions and promote zinc absorption in the body [36]. In addition, another study reported that CycloZ promotes insulin receptor recycling and ameliorates insulin resistance by increasing the intracellular activity of the insulin-degrading enzyme (IDE), a zinc-dependent metalloprotease that degrades insulin [37]. This was consistent with another study that proposed that increased blood IDE level is a risk factor for diabetes and that the inhibition of

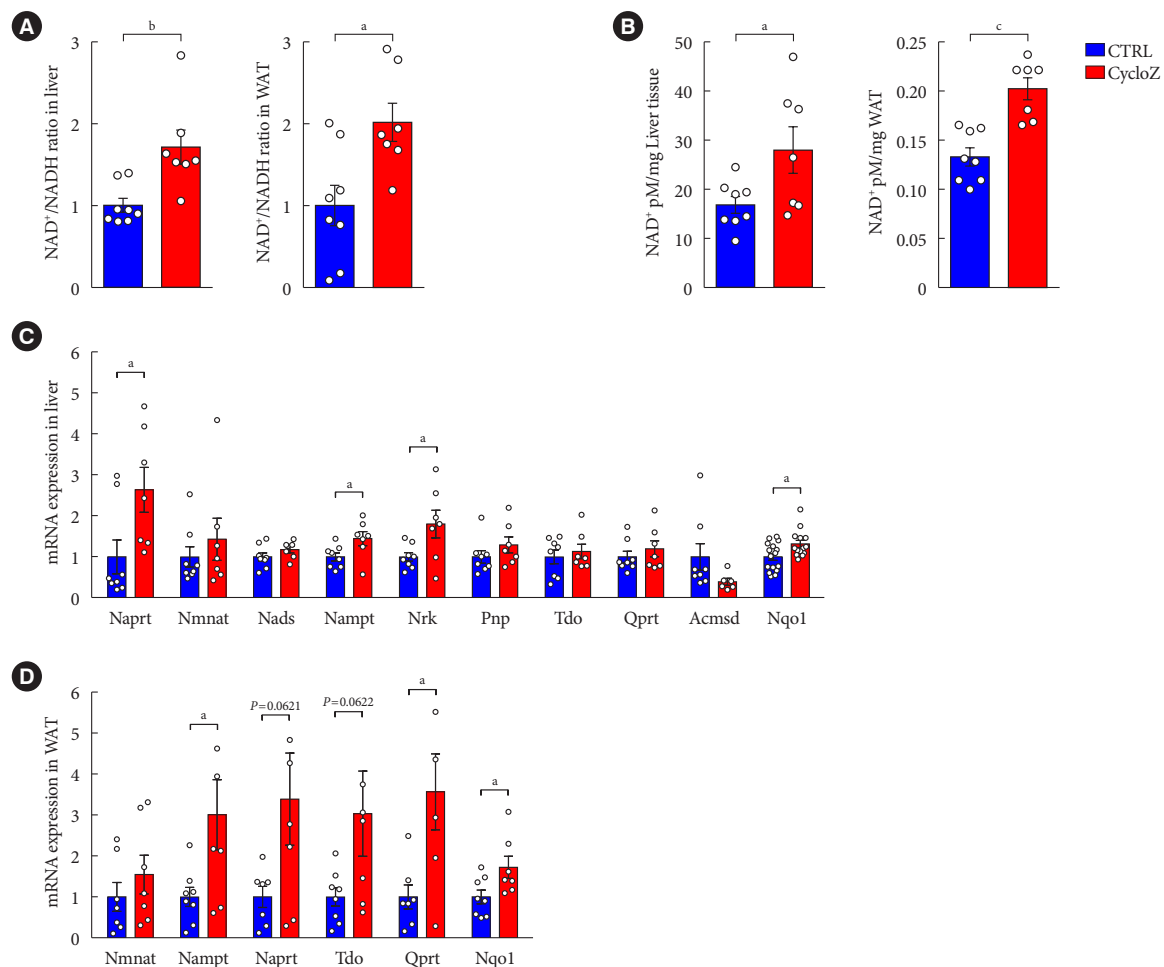


**Fig. 4.** CycloZ administration increases the level of  $\beta$ -nicotinamide adenine dinucleotide (NAD<sup>+</sup>) content by modulating the expression of genes involved in NAD<sup>+</sup> synthesis. (A) NAD<sup>+</sup>/nicotinamide adenine dinucleotide (NADH) ratio in liver and epididymal adipose tissue (EAT) ( $n=7-8$ ). (B) Quantification of NAD<sup>+</sup> in liver and EAT. ( $n=7-8$ ). (C, D) mRNAs expression levels related to NAD<sup>+</sup> synthesis in liver (C) and mesenteric adipose tissue (D) ( $n=7-8$ ). Data shown represent mean  $\pm$  standard error of the mean. Unpaired Student's *t*-tests. CTRL, control; WAT, white adipose tissue; Naprt, nicotinate phosphoribosyltransferase; Nmnat, nicotinamide mononucleotide adenylyltransferase; Nads, NAD synthase; Nampt, nicotinamide phosphoribosyltransferase; Nrk, nicotinamide riboside kinase; Pnp, purine nucleoside phosphorylase; Tdo, tryptophan 2,3-dioxygenase; Qprt, quinolinate phosphoribosyltransferase; Acmsd, aminocarboxymuconate semialdehyde decarboxylase; Nqo1, NAD(P)H quinone dehydrogenase 1. <sup>a</sup> $P \leq 0.05$ , <sup>b</sup> $P \leq 0.01$ , <sup>c</sup> $P \leq 0.001$ .

extracellular IDE can potentially treat diabetes [38]. In clinical studies, it has been reported that zinc supplementation had little to no benefit in T2DM [39,40].

In the present study, we propose a novel mode of action for the anti-diabetic and anti-obesity effects of CycloZ through the modulation of protein acetylation in the liver and VATs of KK-Ay mice. Increase VATs mass have been suggested as one of the major risk factors for various metabolic diseases [41]. In this study, we found a significant reduction in liver and VAT mass

in CycloZ-administered mice. Moreover, PGC-1 $\alpha$  deacetylation upon CycloZ administration induced the transcriptional regulation of genes related to mitochondrial function in the liver and VATs. It has been known that a close relationship exists between PGC-1 $\alpha$  activity and the development of T2DM, which is associated with mitochondria biogenesis and glucose/fatty acid metabolism [42]. Specifically, the reduced activity of PGC-1 $\alpha$  (such as in PGC-1 $\alpha$  G482S) has been linked to altered lipid oxidation [43], and the expression of PGC-1 $\alpha$  in the adi-

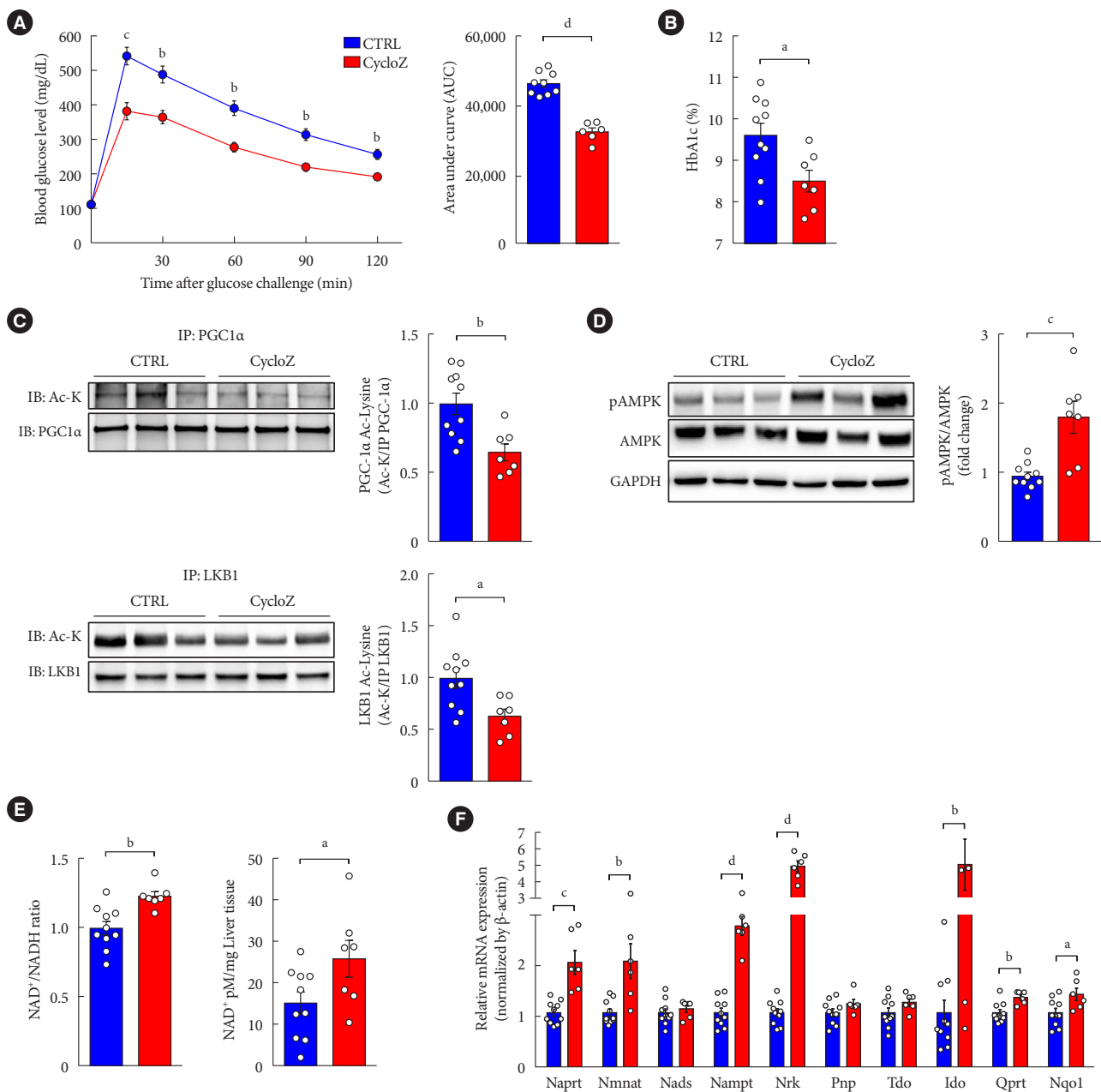


**Fig. 5.** CycloZ administration improves glucose control in a model of severe established type 2 diabetes mellitus. (A) Oral glucose tolerance test for 2 hours after 16 hours fasting and glucose administration (2 g/kg) at 10 weeks of treatment ( $n=8-10$ ). (B) Glycosylated hemoglobin (HbA1c) level at 11 weeks of treatment ( $n=8-10$ ). (C) Acetylated lysine levels on peroxisome proliferator-activated receptor gamma coactivator 1-alpha (PGC-1 $\alpha$ ) and liver kinase B1 (LKB1) in liver ( $n=8-10$ ). (D) Phosphorylated AMP-activated kinase (AMPK) (T172) in liver ( $n=8-10$ ). (E) Increased the level of  $\beta$ -nicotinamide adenine dinucleotide (NAD<sup>+</sup>)/nicotinamide adenine dinucleotide (NADH) ratio and quantification of NAD<sup>+</sup> in liver ( $n=8-10$ ). (F) NAD<sup>+</sup> synthesis related mRNAs expression levels in liver ( $n=8-10$ ). Data shown represent mean  $\pm$  standard error of the mean. Unpaired Student's *t*-tests. CTRL, control; IP, immunoprecipitation; IB, immunoblotting; Ac-K, acetylated-Lysine; GAPDH, glyceraldehyde-3-phosphate dehydrogenase; Naprt, nicotinate phosphoribosyltransferase; Nmnat, nicotinate/nicotinamide mononucleotide adenylyltransferase; Nads, NAD synthase; Nampt, nicotinamide phosphoribosyltransferase; Nrk, Nik related kinase; Pnp, purine nucleoside phosphorylase; Tdo, tryptophan 2,3-dioxygenase; Qprt, quinolinate phosphoribosyltransferase; Nqo1, NAD(P)H quinone dehydrogenase 1. <sup>a</sup> $P \leq 0.05$ , <sup>b</sup> $P \leq 0.01$ , <sup>c</sup> $P \leq 0.001$ , <sup>d</sup> $P \leq 0.0001$ .

pose tissue is downregulated in patient with T2DM [44].

Chronic inflammation with abnormally increased cytokine levels and immune cell infiltration is observed in many metabolic disorders, contributing to disease progression. In the present study, we observed a reduction in the inflammation of the liver and VATs of CycloZ-treated KK-Ay mice. Previous studies have shown that CHP reduces inflammation by regulating NF- $\kappa$ B and Nrf2 signaling or inhibiting NLR family pyrin domain containing 3 (NLRP3) inflammasome production [19,45]. Interestingly, we found that the acetylation of p65, a key NF- $\kappa$ B subunit, decreased upon CycloZ administration. Sirt1 may also have played an important role in reducing inflammation by deacetylating transcription factors such as p65, resulting in the transcriptional repression of various inflammatory genes.

Notably, we showed that CycloZ regulated the expression of enzymes involved in NAD<sup>+</sup> synthesis. Nicotinamide (NAM) is a major contributor to NAD<sup>+</sup> synthesis in mammalian cells. In the classical salvage pathway, nicotinamide phosphoribosyltransferase (NAMPT), a rate-limiting enzyme, converts NAM into nicotinamide mononucleotide (NMN) [46]. The mRNA expression of *Nampt* was increased in both the liver and VATs of CycloZ-treated mice. Since NAMPT is a rate-limiting enzyme, CycloZ treatment increased NAD<sup>+</sup> levels, subsequently increasing Sirt1 activity. The NAD<sup>+</sup>/NADH ratio and the amount of NAD<sup>+</sup> were increased only in the liver and VATs but not in the muscle (Supplementary Fig. 2B), suggesting that CycloZ may modulate NAD<sup>+</sup> synthesis in a tissue-specific manner. We observed increased *Sirt1* mRNA and protein expression in the liver and EAT of mice (Supplementary Fig. 2D and E). SRT1720 and resveratrol, which are known Sirt1 activators, have been reported to increase Sirt1 expression and enzyme activity [47,48]. In our study, it can be inferred that Sirt1 activity may have increased because the NAD<sup>+</sup> level and NAD<sup>+</sup>/NADH ratio, which are essential for Sirt1 activity, were increased. However, further research on whether CycloZ regulates Sirt1 expression is needed to uncover the underlying molecular mechanisms. Together, these data suggest that CycloZ decreases protein acetylation by increasing NAD<sup>+</sup> levels and regulating the activity of NAD<sup>+</sup>-dependent deacetylases such as sirtuins. This warrants future studies on other sirtuin substrates, such as acetyl-CoA synthetase 1 (AceCS1) and histone proteins, and further characterization of the activity of acetyltransferases that control the acetylation status of enzymes related to metabolism.

In general, KK-Ay mice are used as a model of mild hyper-

glycemia to study the prophylactic effects of drugs on T2DM with obesity [17]. However, results from therapeutic studies are essential for the clinical translation of experimental observation. Hyperglycemia in KK-Ay mice worsens with age [18]; therefore, aged KK-Ay mice with advanced hyperglycemia, an animal model of more severe diabetes, were used to examine the therapeutic effect of CycloZ in this study. CycloZ also had a significant anti-diabetic effect in this severe diabetes model, even in the therapeutic mode of administration. Contrary to the results of the prophylactic study, there were no significant changes in body weight and fat weight in mice after CycloZ administration, but their liver weights decreased (Supplementary Fig. 3B-D). According to these results, CycloZ also works effectively on liver fat metabolism and may be used to treat fatty liver disease. Furthermore, CycloZ was well-tolerated in a long-term study in KK-Ay mice (20 weeks) as well as in a 39-week-long toxicology study in beagle dogs (unpublished data). Likewise, initial clinical studies of CycloZ showed no safety issues (NCT00878605, NCT02784275, and NCT03560-271), suggesting that it may have clinical applications in metabolic diseases.

In conclusion, CycloZ activated the Sirt1/PGC-1 $\alpha$ /LKB1/AMPK signaling axis, exhibiting anti-diabetic and anti-obesity properties and an excellent safety profile. Based on these data, we suggest that CycloZ acts as a novel NAD<sup>+</sup> booster and Sirt1 deacetylase activator, a mechanism of action different from traditional T2DM drugs.

## SUPPLEMENTARY MATERIALS

Supplementary materials related to this article can be found online at <https://doi.org/10.4093/dmj.2022.0244>.

## CONFLICTS OF INTEREST

Jongsu Jeon, Dohyun Lee, Bobae Kim, Onyu Park, and Seoyoung Baek are employed by NovMetaPharma. Hoe-Yune Jung and Johan Auwerx are board members of NovMetaPharma.

## AUTHOR CONTRIBUTIONS

Conception or design: J.A., K.T.K., H.Y.J.

Acquisition, analysis, or interpretation of data: J.J., D.L., B.K., B.Y.P., C.J.O., O.P., S.B., C.W.L., H.Y.J.

Drafting the work or revising: M.J.K., J.H.J., I.K.L., D.R., S.F.



J.A., K.T.K., H.Y.J.

Final approval of the manuscript: J.J., D.L., J.A., K.T.K., H.Y.J.

## ORCID

Jongsu Jeon <https://orcid.org/0000-0002-1699-0067>

Dohyun Lee <https://orcid.org/0000-0002-0005-6886>

Johan Auwerx <https://orcid.org/0000-0002-5065-5393>

Kyong-Tai Kim <https://orcid.org/0000-0001-7292-2627>

Hoe-Yune Jung <https://orcid.org/0000-0003-1802-5428>

## FUNDING

This research was supported by a grant of the Korea Health Technology R&D Project through the Korea Health Industry Development Institute (KHIDI), funded by the Ministry of Health & Welfare, Republic of Korea (Grant Number: HI16C1501).

## ACKNOWLEDGMENTS

None

## REFERENCES

1. Galicia-Garcia U, Benito-Vicente A, Jebbari S, Larrea-Sebal A, Siddiqi H, Uribe KB, et al. Pathophysiology of type 2 diabetes mellitus. *Int J Mol Sci* 2020;21:6275.
2. Davies MJ, D'Alessio DA, Fradkin J, Kernan WN, Mathieu C, Mingrone G, et al. Management of hyperglycemia in type 2 diabetes, 2018. a consensus report by the American Diabetes Association (ADA) and the European Association for the Study of Diabetes (EASD). *Diabetes Care* 2018;41:2669-701.
3. Montvida O, Shaw J, Atherton JJ, Stringer F, Paul SK. Long-term trends in antidiabetes drug usage in the U.S.: real-world evidence in patients newly diagnosed with type 2 diabetes. *Diabetes Care* 2018;41:69-78.
4. White JR Jr. A brief history of the development of diabetes medications. *Diabetes Spectr* 2014;27:82-6.
5. Freeland B, Farber MS. Type 2 diabetes drugs: a review. *Home Healthc Now* 2015;33:304-10.
6. Pathak R, Bridgeman MB. Dipeptidyl peptidase-4 (DPP-4) inhibitors in the management of diabetes. *P T* 2010;35:509-13.
7. Garofalo C, Borrelli S, Liberti ME, Andreucci M, Conte G, Minutolo R, et al. SGLT2 inhibitors: nephroprotective efficacy and side effects. *Medicina (Kaunas)* 2019;55:268.
8. Norvell A, McMahon SB. Cell biology: rise of the rival. *Science* 2010;327:964-5.
9. Wang Q, Zhang Y, Yang C, Xiong H, Lin Y, Yao J, et al. Acetylation of metabolic enzymes coordinates carbon source utilization and metabolic flux. *Science* 2010;327:1004-7.
10. Houtkooper RH, Pirinen E, Auwerx J. Sirtuins as regulators of metabolism and healthspan. *Nat Rev Mol Cell Biol* 2012;13:225-38.
11. Menzies KJ, Zhang H, Katsyuba E, Auwerx J. Protein acetylation in metabolism: metabolites and cofactors. *Nat Rev Endocrinol* 2016;12:43-60.
12. Canto C, Auwerx J. PGC-1alpha, SIRT1 and AMPK, an energy sensing network that controls energy expenditure. *Curr Opin Lipidol* 2009;20:98-105.
13. Lan F, Cacicedo JM, Ruderman N, Ido Y. SIRT1 modulation of the acetylation status, cytosolic localization, and activity of LKB1. Possible role in AMP-activated protein kinase activation. *J Biol Chem* 2008;283:27628-35.
14. Vannini N, Campos V, Girotra M, Trachsel V, Rojas-Sutterlin S, Tratwal J, et al. The NAD-booster nicotinamide riboside potentially stimulates hematopoiesis through increased mitochondrial clearance. *Cell Stem Cell* 2019;24:405-18.
15. Zhang H, Ryu D, Wu Y, Gariani K, Wang X, Luan P, et al. NAD<sup>+</sup> repletion improves mitochondrial and stem cell function and enhances life span in mice. *Science* 2016;352:1436-43.
16. Rajman L, Chwalek K, Sinclair DA. Therapeutic potential of NAD-boosting molecules: the in vivo evidence. *Cell Metab* 2018;27:529-47.
17. Wang YW, Sun GD, Sun J, Liu SJ, Wang J, Xu XH, et al. Spontaneous type 2 diabetic rodent models. *J Diabetes Res* 2013;2013:401723.
18. Iwatsuka H, Shino A, Suzuoki Z. General survey of diabetic features of yellow KK mice. *Endocrinol Jpn* 1970;17:23-35.
19. Minelli A, Grottelli S, Mierla A, Pinnen F, Cacciatore I, Bellezza I. Cyclo(His-Pro) exerts anti-inflammatory effects by modulating NF- $\kappa$ B and Nrf2 signalling. *Int J Biochem Cell Biol* 2012;44:525-35.
20. Mizuma T, Masubuchi S, Awazu S. Intestinal absorption of stable cyclic glycylphenylalanine: comparison with the linear form. *J Pharm Pharmacol* 1997;49:1067-71.
21. Jaspán JB, Banks WA, Kastin AJ. Study of passage of peptides across the blood-brain barrier: biological effects of cyclo(His-Pro) after intravenous and oral administration. *Ann N Y Acad Sci* 1994;739:101-7.
22. Prasad C. Cyclo(His-Pro): its distribution, origin and function

- in the human. *Neurosci Biobehav Rev* 1988;12:19-22.
23. Song MK, Hwang IK, Rosenthal MJ, Harris DM, Yamaguchi DT, Yip I, et al. Anti-hyperglycemic activity of zinc plus cyclo (his-pro) in genetically diabetic Goto-Kakizaki and aged rats. *Exp Biol Med* (Maywood) 2003;228:1338-45.
  24. Song MK, Rosenthal MJ, Song AM, Uyemura K, Yang H, Ament ME, et al. Body weight reduction in rats by oral treatment with zinc plus cyclo-(His-Pro). *Br J Pharmacol* 2009;158:442-50.
  25. Hwang IK, Go VL, Harris DM, Yip I, Kang KW, Song MK. Effects of cyclo (his-pro) plus zinc on glucose metabolism in genetically diabetic obese mice. *Diabetes Obes Metab* 2003;5:317-24.
  26. Jung HY, Kim B, Ryu HG, Ji Y, Park S, Choi SH, et al. Amodiaquine improves insulin resistance and lipid metabolism in diabetic model mice. *Diabetes Obes Metab* 2018;20:1688-701.
  27. Kim HJ, Kim JY, Lee SJ, Kim HJ, Oh CJ, Choi YK, et al.  $\alpha$ -Lipoic acid prevents neointimal hyperplasia via induction of p38 mitogen-activated protein kinase/Nur77-mediated apoptosis of vascular smooth muscle cells and accelerates postinjury reendothelialization. *Arterioscler Thromb Vasc Biol* 2010;30:2164-72.
  28. Yeung F, Hoberg JE, Ramsey CS, Keller MD, Jones DR, Frye RA, et al. Modulation of NF-kappaB-dependent transcription and cell survival by the SIRT1 deacetylase. *EMBO J* 2004;23:2369-80.
  29. Berthiaume JM, Hsiung CH, Austin AB, McBrayer SP, Depuydt MM, Chandler MP, et al. Methylene blue decreases mitochondrial lysine acetylation in the diabetic heart. *Mol Cell Biochem* 2017;432:7-24.
  30. Kosanam H, Thai K, Zhang Y, Advani A, Connelly KA, Diamandis EP, et al. Diabetes induces lysine acetylation of intermediary metabolism enzymes in the kidney. *Diabetes* 2014;63:2432-9.
  31. Finkel T, Deng CX, Mostoslavsky R. Recent progress in the biology and physiology of sirtuins. *Nature* 2009;460:587-91.
  32. Katsyuba E, Romani M, Hofer D, Auwerx J. NAD<sup>+</sup> homeostasis in health and disease. *Nat Metab* 2020;2:9-31.
  33. Kinlaw WB, Levine AS, Morley JE, Silvis SE, McClain CJ. Abnormal zinc metabolism in type II diabetes mellitus. *Am J Med* 1983;75:273-7.
  34. Failla ML, Gardell CY. Influence of spontaneous diabetes on tissue status of zinc, copper, and manganese in the BB Wistar rat. *Proc Soc Exp Biol Med* 1985;180:317-22.
  35. Zhao Y, Tan Y, Dai J, Wang B, Li B, Guo L, et al. Zinc deficiency exacerbates diabetic down-regulation of Akt expression and function in the testis: essential roles of PTEN, PTP1B and TRB3. *J Nutr Biochem* 2012;23:1018-26.
  36. Rosenthal MJ, Hwang IK, Song MK. Effects of arachidonic acid and cyclo (his-pro) on zinc transport across small intestine and muscle tissues. *Life Sci* 2001;70:337-48.
  37. Song MK, Bischoff DS, Song AM, Uyemura K, Yamaguchi DT. Metabolic relationship between diabetes and Alzheimer's Disease affected by Cyclo(His-Pro) plus zinc treatment. *BBA Clin* 2016;7:41-54.
  38. Tang WJ. Targeting insulin-degrading enzyme to treat type 2 diabetes mellitus. *Trends Endocrinol Metab* 2016;27:24-34.
  39. El Dib R, Gameiro OL, Ogata MS, Modolo NS, Braz LG, Jorge EC, et al. Zinc supplementation for the prevention of type 2 diabetes mellitus in adults with insulin resistance. *Cochrane Database Syst Rev* 2015;5:CD005525.
  40. Jayawardena R, Ranasinghe P, Galappaththy P, Malkanthi R, Constantine G, Katulanda P. Effects of zinc supplementation on diabetes mellitus: a systematic review and meta-analysis. *Diabetol Metab Syndr* 2012;4:13.
  41. Fox CS, Massaro JM, Hoffmann U, Pou KM, Maurovich-Horvat P, Liu CY, et al. Abdominal visceral and subcutaneous adipose tissue compartments: association with metabolic risk factors in the Framingham Heart Study. *Circulation* 2007;116:39-48.
  42. Hara K, Tobe K, Okada T, Kadowaki H, Akanuma Y, Ito C, et al. A genetic variation in the PGC-1 gene could confer insulin resistance and susceptibility to type II diabetes. *Diabetologia* 2002;45:740-3.
  43. Muller YL, Bogardus C, Pedersen O, Baier L. A Gly482Ser missense mutation in the peroxisome proliferator-activated receptor gamma coactivator-1 is associated with altered lipid oxidation and early insulin secretion in Pima Indians. *Diabetes* 2003;52:895-8.
  44. Hammarstedt A, Jansson PA, Wesslau C, Yang X, Smith U. Reduced expression of PGC-1 and insulin-signaling molecules in adipose tissue is associated with insulin resistance. *Biochem Biophys Res Commun* 2003;301:578-82.
  45. Grottelli S, Mezzasoma L, Scarpelli P, Cacciatore I, Cellini B, Bellezza I. Cyclo(His-Pro) inhibits NLRP3 inflammasome cascade in ALS microglial cells. *Mol Cell Neurosci* 2019;94:23-31.
  46. Li XQ, Lei J, Mao LH, Wang QL, Xu F, Ran T, et al. NAMPT and NAPRT, key enzymes in NAD salvage synthesis pathway, are of negative prognostic value in colorectal cancer. *Front Oncol* 2019;9:736.

47. Sacitharan PK, Bou-Gharios G, Edwards JR. SIRT1 directly activates autophagy in human chondrocytes. *Cell Death Discov* 2020;6:41.
48. Ling L, Gu S, Cheng Y. Resveratrol inhibits adventitial fibroblast proliferation and induces cell apoptosis through the SIRT1 pathway. *Mol Med Rep* 2017;15:567-72.